

Increased Beta2-Adrenoceptors in Doxorubicin-Induced Cardiomyopathy in Rat

Nolwenn Merlet^{1,2}, Nicolas Piriou^{1,3}, Bertrand Rozec^{1,4}, Amandine Grabherr¹, Benjamin Lauzier^{1,2}, Jean-Noël Trochu^{1,2,3}, Chantal Gauthier^{1,2*}

1 Institut du thorax, Unité Inserm UMR 1087/CNRS UMR 6291, Nantes, France, **2** Université de Nantes, Nantes, France, **3** CHU Nantes, l'institut du thorax, Nantes, France, **4** CHU Nantes, Department of Anaesthesiology, Nantes, France

Abstract

Background: The toxicity of doxorubicin, leading to an irreversible heart failure, limits its use as chemotherapeutic agent. The beneficial effects of early administration of β -blocker were reported in patients with heart failure due to doxorubicin, suggesting an important role of β -adrenoceptors (β -ARs). This study aimed to identify a putative target (β -AR and/or its effectors) at the early phase of a chronic doxorubicin-induced cardiomyopathy (Dox-CM) in a rat model.

Methodology: Dox-CM was induced by six doxorubicin injections (cumulative dose: 15 mg.kg⁻¹) and validated by echocardiography and left ventricle (LV) catheterization. The β -AR protein expressions in LV were evaluated by western-blot at days 35 (d35) and 70 (d70) after the first doxorubicin injection. *Ex vivo* cardiac contractility (dP/dt_{max}, dP/dt_{min}) was evaluated on isolated heart in response to specific β -AR stimulations at d35.

Results: At d35, Dox-CM hearts were characterized by mild LV systolic and diastolic dysfunctions, which were exacerbated at d70. In Dox-CM hearts, β_3 -AR expression was only decreased at d70 (-37±8%). At d35, β_1 -AR expression was decreased by 68±6%, but *ex vivo* β_1 -AR function was preserved due to, at least in part, an increased adenylyl cyclase response assessed by forskolin. β_2 -AR expression was increased both at d35 (+58±22%) and d70 (+174±35%), with an increase of *ex vivo* β_2 -AR response at d35. Inhibition of Gi protein with pertussis toxin did not affect β_2 -AR response in Dox-CM hearts, suggesting a decoupling of β_2 -AR to Gi protein.

Conclusion: This study highlights the β_1/β_2 -AR imbalance in early Dox-CM and reveals the important role that β_2 -AR/Gi coupling could play in this pathology. Our results suggest that β_2 -AR could be an interesting target at early stage of Dox-CM.

Citation: Merlet N, Piriou N, Rozec B, Grabherr A, Lauzier B, et al. (2013) Increased Beta2-Adrenoceptors in Doxorubicin-Induced Cardiomyopathy in Rat. PLoS ONE 8(5): e64711. doi:10.1371/journal.pone.0064711

Editor: Philippe Rouet, I2MC INSERM UMR U1048, France

Received: January 29, 2013; **Accepted:** April 17, 2013; **Published:** May 31, 2013

Copyright: © 2013 Merlet et al. This is an open-access article distributed under the terms of the Creative Commons Attribution License, which permits unrestricted use, distribution, and reproduction in any medium, provided the original author and source are credited.

Funding: This work was supported by the "Association Française contre les Myopathies", the "Fédération Française de Cardiologie", the "Fondation de France" and the "Fondation Genavie". The funders had no role in study design, data collection and analysis, decision to publish, or preparation of the manuscript.

Competing Interests: The authors have declared that no competing interests exist.

* E-mail: chantal.gauthier@univ-nantes.fr

Introduction

Anthracyclines, like doxorubicin (Dox), epirubicin and daunorubicin, are among the most effective drugs used in chemotherapy for cancer patients. Since the late 60s, Dox is frequently used against a variety of cancers including Hodgkin's lymphoma [1], soft-tissue sarcomas [2], leukemia and solid tumors. However, Dox administration is limited due to severe cardiotoxic effects leading to dilated cardiomyopathy [3]. Prognosis of heart failure (HF) due to Dox-cardiotoxicity is poor and even worse than ischemic or idiopathic dilated cardiomyopathy. Although several mechanisms have been proposed to describe the mechanisms by which Dox induces cardiotoxicity (generation of free radicals, mitochondrial disruption, alteration of cellular energetic, and initiation of apoptotic cascades), these mechanisms are still not fully understood [4–6] and there is no specific treatment for Dox-induced cardiomyopathy (Dox-CM) [6,7]; treatments classically used for other HFs with systolic dysfunction induce only limited beneficial effects in Dox-CM.

As in different HF etiologies, Dox-CM is characterized by an alteration of adrenergic system [8]. However, at the present time, only few studies have examined the role of cardiac β_1 - and β_2 -adrenoceptor (β -AR) subtypes in the pathogenesis of Dox-cardiotoxicity [9,10] and only one study, at late-onset Dox-CM, assessed β_3 -AR subtype [11], which is recently described as a new target for some β -blockers such as nebivolol [12,13]. Despite this lack in experimental data, some clinical studies investigated β -blocker therapies in Dox-CM. Kalay *et al.*, demonstrated that left ventricular (LV) diameters remained constant and diastolic function was better preserved after Dox-treatment in patients receiving carvedilol, compared to placebo [14]. However, Georgakopoulos *et al.*, demonstrated that metoprolol, a β -blocker without antioxidant properties, failed to give cardioprotection in lymphoma-treated doxorubicin patients [15]. It was reported that an early start of treatment with angiotensin-converting enzyme inhibitors (ACEIs), in association or not with β -blockers, both improves myocardial contractility [16] and patients' prognosis

Table 1. Antibodies used for western-blot.

Protein	Primary antibody		Secondary antibody	
	Description	Dilution	Description	Dilution
β_1 -AR	Rabbit polyclonal antibody, Sigma-Aldrich (A-272)	1/2,000	Goat anti-rabbit immunoglobulin G, Santa-Cruz Biotechnology (sc-2054)	1/10,000
β_2 -AR	Rabbit polyclonal antibody, AbCam Ltd (ab36956)	1/2,000	Goat anti-rabbit immunoglobulin G, Santa-Cruz Biotechnology (sc-2054)	1/15,000
β_3 -AR	Rabbit polyclonal antibody, Santa Cruz Biotechnology (sc-50436)	1/5,000	Goat anti-rabbit immunoglobulin G, Santa-Cruz Biotechnology (sc-2054)	1/15,000
G α	Rabbit polyclonal antibody, Merk Chemicals Ltd (371732)	1/1,000	Goat anti-rabbit immunoglobulin G, Santa-Cruz Biotechnology (sc-2054)	1/10,000
G α_2	Rabbit polyclonal antibody, Merk Chemicals Ltd (371727)	1/5,000	Goat anti-rabbit immunoglobulin G, Santa-Cruz Biotechnology (sc-2054)	1/10,000
GAPDH	Mouse monoclonal antibody, Santa-Cruz Biotechnology (sc-32233)	1/10,000	Goat anti-mouse immunoglobulin G, Santa-Cruz Biotechnology (sc-2055)	1/50,000

Primary antibodies were diluted in *TBS-T*, excepted for G α_2 protein detection which was diluted in 5% non-fat dry milk in *TBS-T*. All secondary antibodies were diluted in 1% non-fat dry milk in *TBS-T*.

doi:10.1371/journal.pone.0064711.t001

[17]. Although the exact mechanism is still poorly understood, the authors highlighted the importance of an early diagnosis, because a delayed treatment (>6 months after the end of chemotherapy) is inefficient [17].

The aim of the present study was to identify a putative target (β -AR and/or its effectors) involved at the early phase of a chronic Dox-CM in a rat model. This study demonstrated for the first time that β_2 -AR expression was increased from 35 days after the first Dox-injection, this effect was maintained until 70 days after the first Dox-injection, resulting in an increase of β_2 -AR-induced contractility. In addition, β_1 -AR function was preserved, in spite of decreased β_1 -AR protein expression. This discrepancy could be explained by an increase of adenylyl cyclase (AC) expression and/or activity as illustrated by an increased forskolin-induced response in Dox-CM rats.

Methods

Ethics Statement

All experiments were performed in accordance with the 1996 Guide for the Care and Use of Laboratory Animals published by the U.S. National Institute of Health. The protocol was approved by the Direction Départementale de la Protection des Populations (agreement number C-44 015) and all efforts were made to minimize suffering.

Animal Model

One hundred and fifty eight male Sprague-Dawley rats (225–250 g) were purchased from Janvier (Le Genest St Isle, France) and were housed under standard conditions of room temperature, humidity (40–60%) and 12 h light/dark cycle. Food and water were available *ad libitum*.

Doxorubicin (Adriblastine® 50 mg/25 mL, Pfizer, France) was administered intraperitoneally in six equal injections (each containing 2.5 mg.kg⁻¹) over a period of two weeks, with a total cumulative dose of 15 mg.kg⁻¹ body weight (Dox-CM: n = 100). Age-matched rats injected with saline were used as controls (Ctrl: n = 58). Rats were then bred in animal housing until three weeks after the last injection (day 35 (d35); Ctrl: n = 46, Dox-CM: n = 76) or until eight weeks after the last injection (day 70 (d70); Ctrl: n = 12, Dox-CM: n = 24). At d35, twenty Dox-CM rats and twenty Ctrl rats were randomly selected to be hemodynamically explored

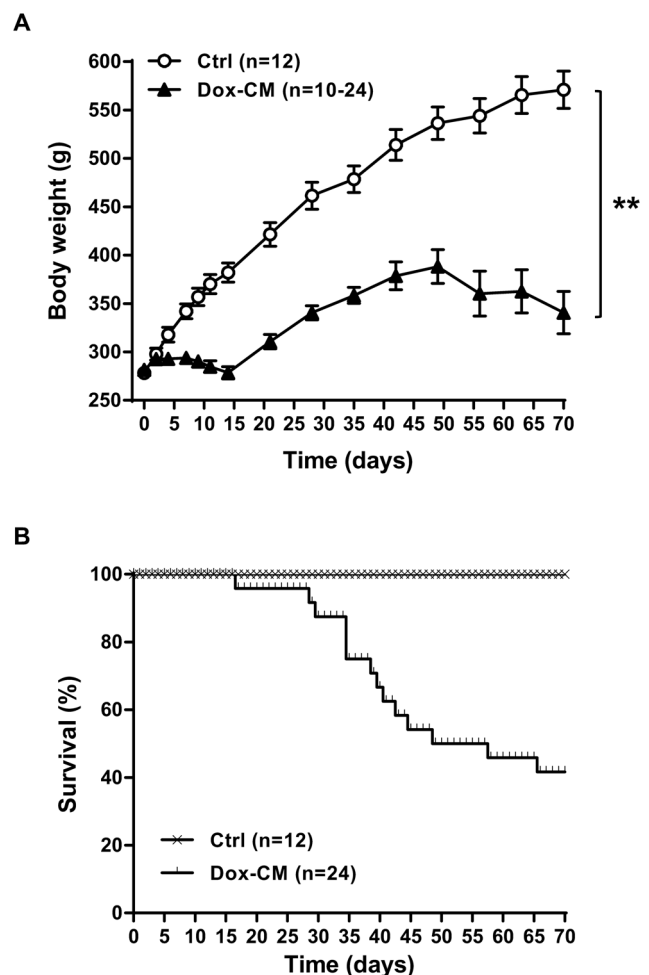


Figure 1. Body weight (A) and survival curves (B) of Ctrl and Dox-CM rats. Values are means \pm sem **: $P < 0.001$ vs Ctrl. Ctrl: control, Dox-CM: Doxorubicin-induced cardiomyopathy. doi:10.1371/journal.pone.0064711.g001

Table 2. Cardiac morphological parameters in Ctrl and Dox-CM rats, at d35 and d70.

Parameters	d35		d70	
	Ctrl (n = 30)	Dox-CM (n = 34)	Ctrl (n = 12)	Dox-CM (n = 10)
Body wt (g)	516±7	395±6**	571±19	341±22**
Heart wt (mg)	1445±31	1112±17**	1317±24	879±51**
LV wt (mg)	729±17	562±11**	755±16	483±28**
Heart wt/Body wt (mg.g ⁻¹)	2.80±0.03	2.82±0.04	2.32±0.04	2.60±0.07*
LV wt/Body wt (mg.g ⁻¹)	1.41±0.02	1.43±0.02	1.33±0.04	1.43±0.05
Heart wt/Tibia length (mg.cm ⁻¹)	272±5	218±3**	239±4	166±9**
LV wt/Tibia length (mg.cm ⁻¹)	137±3	110±2**	137±3	92±5**

Ctrl: control; Dox-CM: Doxorubicin-induced cardiomyopathy; LV: left ventricle; wt: weight. Values are means ± sem. *: $P < 0.05$ vs respective Ctrl. **: $P < 0.001$ vs respective Ctrl.

doi:10.1371/journal.pone.0064711.t002

by echocardiography-Doppler. Then either rats were hemodynamically assessed by LV catheterization, or rat hearts were removed either to test *ex vivo* cardiac contractile function or to perform biochemical studies. At d70, rats were used to perform echocardiography-Doppler and biochemical studies.

Echocardiography-Doppler

Transthoracic echocardiography was performed using a commercially available ultrasound system (VIVID7, GE Healthcare, Horton, Norway) equipped with a 10 MHz sectorial probe. Rats were anaesthetized with a gas-mixture of 1% isoflurane (Forene®, Abbott France, Rungis, France) in O₂. The chest was shaved and the animal was positioned on a heating pad in a supine position. All recordings were monitored under a continuous single-channel electrocardiogram obtained on the imaging system by fixing the electrodes to the limbs. Using two-dimensional imaging, a short axis view of the LV at the level of the papillary muscles was obtained and the two-dimensionally guided M-mode recording through the anterior and posterior walls of the LV was taken as recommended by the American Society of Echocardiography [18]. Then, trans-mitral inflow in pulsed-wave Doppler from apical four chamber view and tissue Doppler imaging (TDI) on basal segments of septal and lateral walls in apical four chamber view were taken as previously described [19]. A cine-loop of LV parasternal short axis view with high frame rate was obtained. All acquisitions were performed by the same operator.

All images were digitally stored on hard disks for off-line analysis (EchoPac Q-analysis software, GE Healthcare). Measurements were made on five cardiac cycles and averaged for each data value. The following parameters were determined as recommended by the American Society of Echocardiography [18]: LV end diastolic and systolic diameters (LVEDD and LVESD), diastolic posterior wall thicknesses (dpWth). LV end diastolic and systolic volumes (LVEDV and LVESV) were calculated from the Teichholz method in order to assess LV ejection fraction (LVEF), whereas LV shortening fraction (LVSF) was calculated from LVEDD and LVESD previously measured. LV diastolic function parameters were derived from pulsed-wave trans-mitral inflow pattern and TDI off-line analyses as previously described [20]: the peak of E wave velocities, the isovolumic relaxation time (IVRT), the mean of peak velocities of basal septal and lateral walls (pulsed wave TDI) during systole (Sa) and in early diastole (Ea) to calculate E/Ea ratio. Radial 2D strain analyses were performed using the

2D speckle-tracking method on every medial myocardial segment [21].

Left Ventricle Catheterization

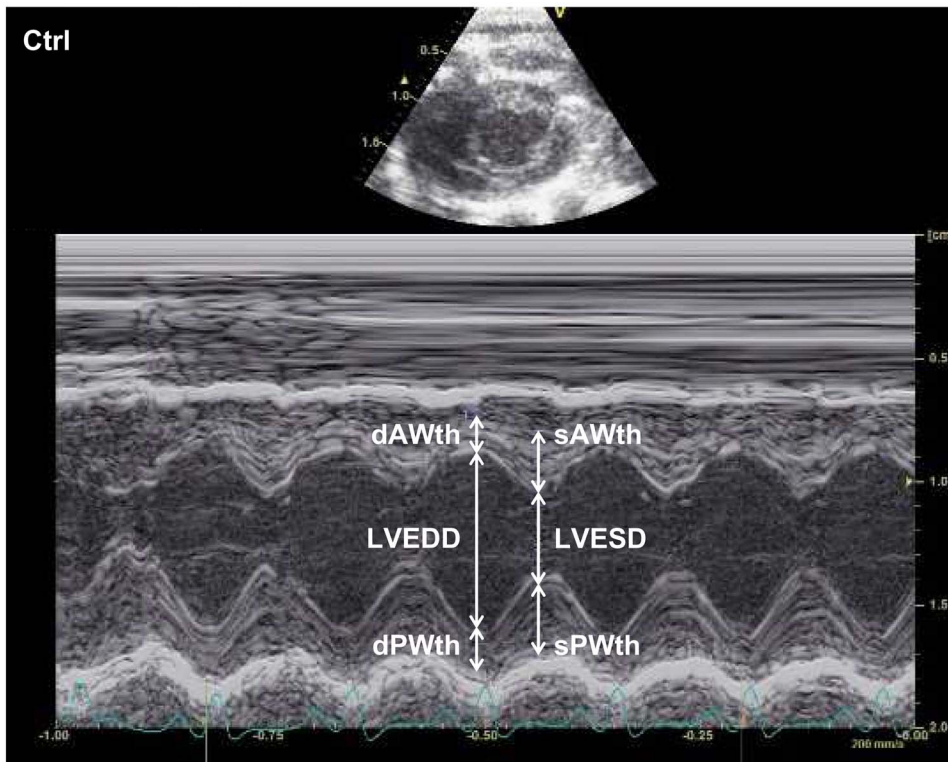
LV catheterization was performed, at d35, by a 2F microtip pressure catheter (SPR 838, Millar instruments Inc, Houston, Texas). Anaesthesia maintenance on spontaneously breathing rats was performed with an inhalational anaesthesia system for small animal (TEM anaesthesia, Lormont, France). Isoflurane was delivered through a nose mask at a concentration of 2% volume and 1 L.min⁻¹ O₂ flow to limit hemodynamic repercussion. Body temperature was monitored by rectal probe and maintained constant (37°C) by warming-blanket. The right carotid artery was isolated, ligated at the proximal part and the pressure catheter was inserted in. Signals were recorded using an Analogic/Digital converter (EMKA Technologies, Paris, France), stored and displayed on a computer by the IOX1.5.7 Software System (EMKA Technologies). Data were analysed using Datanalyst software (EMKA Technologies). The following parameters were obtained: LV end diastolic pressure (LVEDP), LV contraction and relaxation velocities (dP/dt_{max} and dP/dt_{min}, respectively), the index of LV relaxation constant (Tau).

The animals were thereafter sacrificed by injection of a pentobarbital overdose.

Western-blot

The expressions of β_1 -AR, β_2 -AR, β_3 -AR, Gs α , Gi α_2 and GAPDH were examined by western-blot, at d35 and d70. Hearts were rapidly isolated and placed in a cold Tyrode solution composed as followed (in mM): NaCl, 137; KCl, 5.4; MgCl₂, 1.2; Na₂HPO₄, 1.2; Hepes, 20; CaCl₂, 1.0; pH 7.4 (Sigma-Aldrich, St Quentin Fallavier, France). LV and septum free walls were carefully separated and frozen in liquid nitrogen and stored at -80°C until used. LV and septum free walls samples were homogenized in 3 mL of Ripa buffer for 1 g of tissue plus 1X PMSF (Interchim, Montluçon, France) and 2X protease inhibitor cocktail (Roche, Mannheim, Germany). Protein samples (25 μ g) were submitted to electrophoresis on a 10% polyacrylamide/sodium dodecyl sulfate gel and then were run 150 min at 20 mA per membrane in TG-SDS buffer (Interchim). Gels and nitrocellulose membranes (Hybond C super membrane, Amersham, Saclay, France) were equilibrated in TG-SDS buffer with 20% ethanol, and protein fractions were transferred using an electroblotting apparatus (Bio-Rad, Marnes La Coquette, France). Nonspecific

A



B

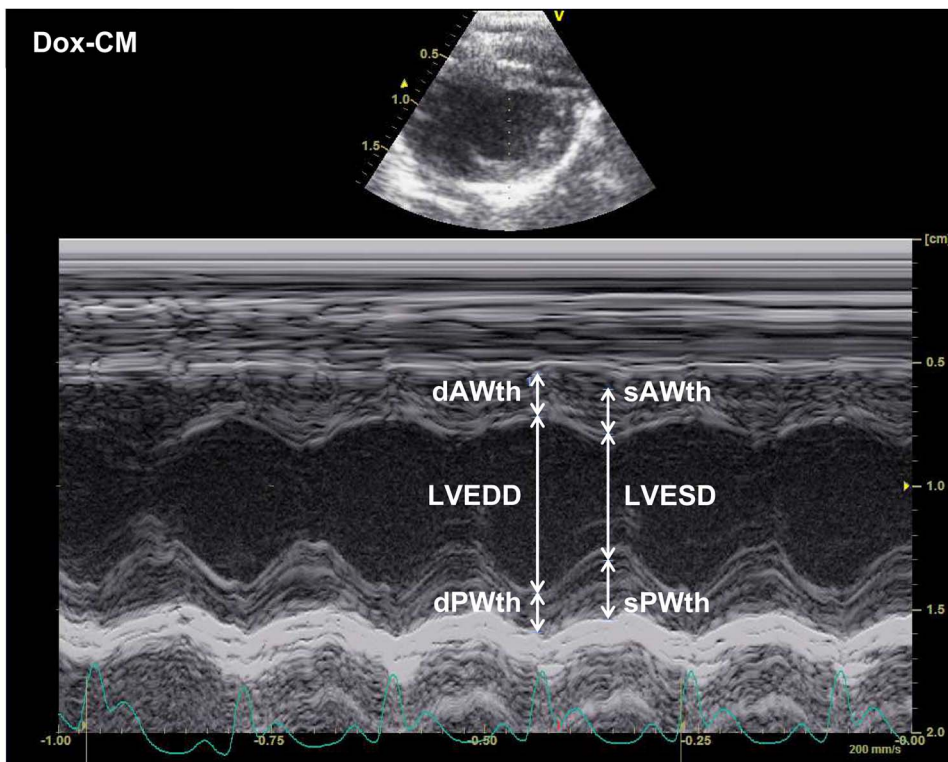


Figure 2. Representative images obtained by echocardiography at day 35 in Ctrl (A) and Dox-CM (B) rats. Images were obtained with a short axis view of a two-dimensionally directed M-mode. Ctrl: control, dAWth: diastolic anterior wall thickness, Dox-CM: Doxorubicin-induced cardiomyopathy, dPWth: diastolic posterior wall thickness, LVEDD: left ventricular end diastolic diameter, LVESD: left ventricular end systolic diameter, sAWth: systolic anterior wall thickness, sPWth: systolic posterior wall thickness.
doi:10.1371/journal.pone.0064711.g002

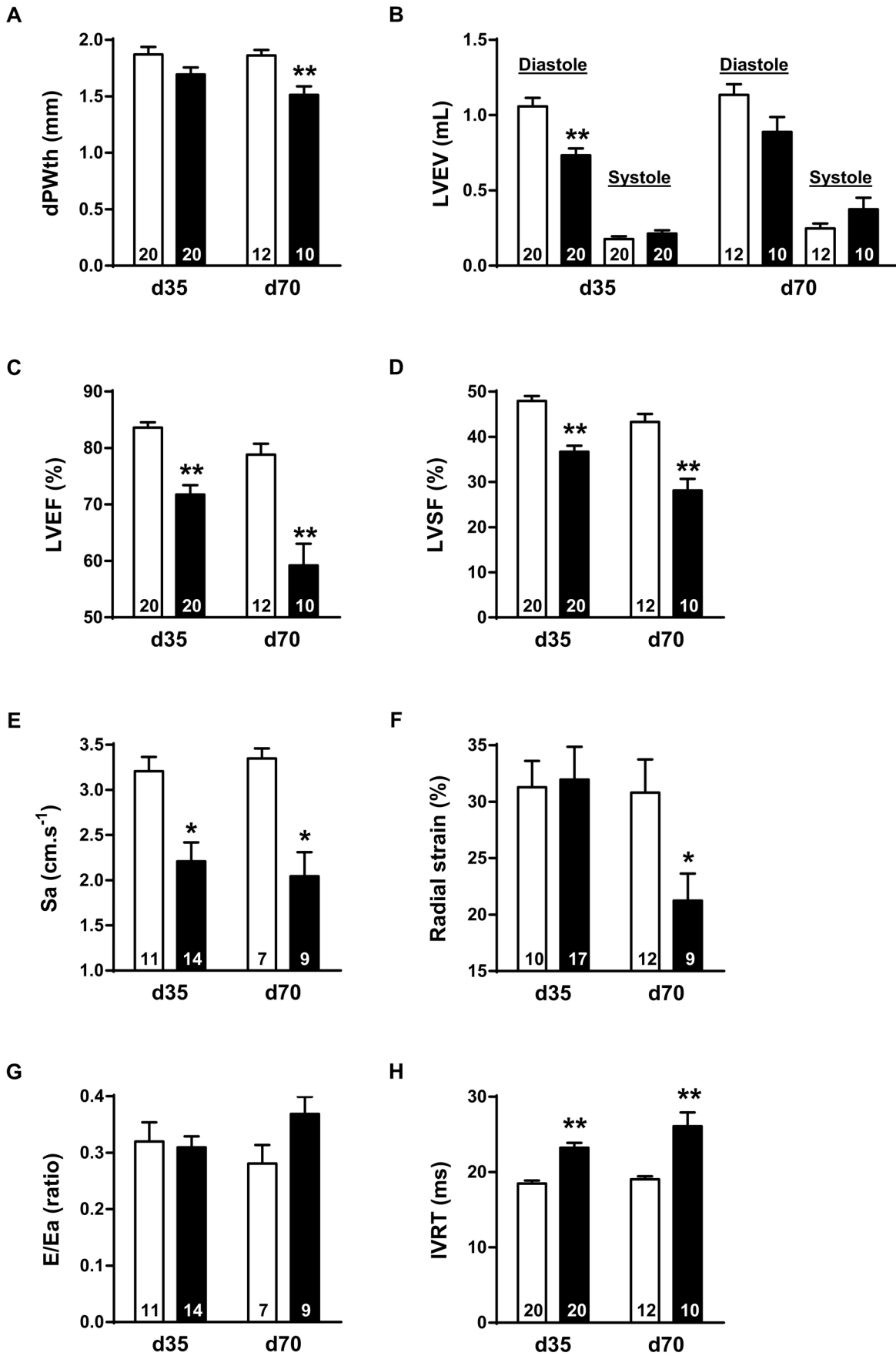


Figure 3. *In vivo* cardiac parameters obtained by echocardiography-Doppler in Ctrl and Dox-CM rats. Ctrl are showed in empty bar and Dox-CM in full bar. Values are means \pm sem *: $P < 0.05$ vs respective Ctrl **: $P < 0.001$ vs respective Ctrl. d35: day 35, d70: day 70, Dox-CM: Doxorubicin-induced cardiomyopathy, dPwth: diastolic posterior wall thickness; E: E wave velocity; Ea: peak velocity of basal and lateral walls in early diastole; IVRT: isovolumic relaxation time; LV: left ventricle; LVEF: left ventricular ejection fraction; LVEV: left ventricular end volume; LVSF: left ventricular shortening fraction; Sa: peak velocity of basal and lateral walls in systole.
doi:10.1371/journal.pone.0064711.g003

binding was blocked by incubating membranes in 5% non-fat dry milk in Tris-buffered saline (TBS) (200 mM Trizma base, 1.4 M NaCl, pH = 7.5) with 0.1% Tween 20 added (TBS-T) and then membranes were incubated with the primary antibody. Membranes were washed in 5% non-fat dry milk in TBS-T and hybridized with the secondary antibody in 1% non-fat dry milk in TBS-T. Finally, membranes were washed with 5% non-fat dry milk in TBS-T then TBS, and antibody complexes were revealed by the enhanced chemiluminescence detection process (Bio-Rad). Chemiluminescence was visualized using an Amersham ImageQuant RT-ECL camera (GE Healthcare) and band signals were assessed by densitometry with ImageQuant TL software (GE Healthcare). For each lane, a ratio to the corresponding GAPDH band intensity was calculated; the use of GAPDH as reference was validated by checking the abundance stability of GAPDH protein between Ctrl and Dox-CM groups.

Antibody references and conditions used in this study are summarized in Table 1.

Whole Heart Contractility

At d35, after removal, hearts were quickly flushed into a cold Tyrode buffer, and then were mounted on a cannula *via* the aorta on a Langendorff apparatus (EMKA Technologies) and perfused with a Krebs-modified solution (in mM: NaCl, 116; KCl, 5; MgSO₄, 1.1; NaH₂PO₄, 0.35; NaHCO₃, 27; glucose, 10; mannitol, 16; Na-Pyruvate, 2; CaCl₂, 1.8) continuously oxygenated with a 95% O₂, 5% CO₂ gas mixture to maintain a pH 7.4. Hearts were perfused at a constant flow-rate of 14 mL.min⁻¹ at 37.0 \pm 0.4°C. After heart beatings became regular, left auricle was gently cut off to insert a small latex balloon, connected to a pressure transducer to record LV pressure, into the LV *via* mitral valves. Before starting record, the minimum pressure into the balloon was adjusted to 8–15 mmHg. Cardiac parameters were recorded using IOX1.5.7 software (EMKA Technologies): inotropism, lusitropism and chronotropism were respectively evaluated by measuring the contraction velocity (dP/dt_{max}), the relaxation velocity (dP/dt_{min}) and the heart rate (HR). After the stabilization

period, specific β_1 -, β_2 - or β_3 -AR functions and AC stimulation were assessed by constructing concentration-response curves to different pharmacological agents. Thus, β_1 - and β_2 -AR functions were assessed by perfusing isoproterenol (a non selective β -AR agonist, 10⁻⁹ to 10⁻⁵ M) in the presence of 10⁻⁶ M L-748,337 (a selective β_3 -AR antagonist) associated to 10⁻⁶ M ICI-118,551 (a selective β_2 -AR antagonist) or to 10⁻⁶ M CGP-20712A (a selective β_1 -AR antagonist), respectively. β_3 -AR function was assessed by perfusing growing concentrations (10⁻⁹ to 10⁻⁵ M) of SR 58611A (a β_3 -AR agonist) and AC response was assessed by perfusing growing concentrations (3.10⁻⁸ to 10⁻⁵ M) of forskolin (an AC activator). In order to assess the role of Gi in the β_2 -AR pathway, we used pertussis toxin (PTX) (a selective Gi inhibitor). Classically, PTX is administered to rats two or three days before experiments [22]. However, due to high mortality in Dox-CM rats pre-treated with PTX, we were not able to apply this protocol and used another one consisting in pre-treating heart with PTX (4 μ g.L⁻¹) in a closed system during 30 min, as described by other groups [23]. Data were analysed using Datanalyst software (EMKA Technologies). After Langendorff experiments, hearts were weighed, as well as LV free walls which were carefully separated from the heart.

Data Analysis and Statistics

Data are presented as means \pm standard error to the mean (sem) of n experiments obtained from n different animals. *In vivo* and *ex vivo* cardiac parameters in baseline as well as protein expressions were compared using Student's *t* test for unpaired data. Concentration-response curves were compared with a two-way ANOVA (concentration, treatments) for repeated measures followed, when appropriated, by a Bonferroni's multiple comparisons test. Differences were considered significant if $P < 0.05$.

Drugs and Chemicals

ICI-118,551, ((\pm)-*erythro*-(S*,S*)-1-[2,3-(Dihydro-7-methyl-1*H*-inden-4-yl)oxy]-3-[(1-methylethyl)amino]-2-butanolhydrochloride), CGP-20712A, 1-[2-[(3-Carbamoyl-4-hydroxy)phenoxy]ethylamino]-3-[4-(1-methyl-4-trifluoromethyl-2-imidazolyl)phenoxy]-2-propanol dihydro chloride, L-748,337, *N*-[[3-[(2*S*)-2-Hydroxy-3-[[2-[4-[(phenylsulfonyl)amino]phenyl]ethyl]amino]propoxy]phenyl]methyl]-acetamide, forskolin and PTX were obtained from Tocris Bioscience (Bristol, UK), isoproterenol was obtained from Sigma-Aldrich (St Quentin Fallavier, France) and SR 58611A, [(RS)-*N*-[(2*S*)-7-ethoxycarbonylmethoxy-1,2,3,4-tetrahydronaphth-2-yl]-(2)-2-(3-chlorophenyl)-2 hydroethanamide hydrochloride] was a generous gift from Sanofi-Synthelabo (Montpellier, France). All drugs were dissolved in distilled water, excepted isoproterenol which was solubilised in 1% acid ascorbic and L-748,337 and forskolin which were solubilised in dimethylsulfoxide (Sigma-Aldrich). The final concentration of the solvent in the organ bath was less than 0.1% v.v⁻¹ and was used as controls for the effect of the active drug.

Results

Mortality and General Characteristics of Animals

Dox-CM rats did not gain weight during the Dox-treatment, whereas the body weight of Ctrl rats increased regularly. After the

Table 3. *In vivo* cardiac parameters obtained by LV catheterization in Ctrl and Dox-CM rats, at d35.

Parameters	Ctrl (n = 10)	Dox-CM (n = 16)
Heart rate (bpm)	325 \pm 10	366 \pm 9*
LV contractility		
dP/dt _{max} (mmHg.s ⁻¹)	5782 \pm 425	5749 \pm 330
LV diastolic function		
Tau (ms)	9.30 \pm 0.26	8.38 \pm 0.20*
dP/dt _{min} (mmHg.s ⁻¹)	-5649 \pm 511	-5861 \pm 306
LV loading conditions		
LVEDP (mmHg)	8.10 \pm 1.03	6.69 \pm 0.60

Ctrl: control; Dox-CM: Doxorubicin-induced cardiomyopathy; dP/dt_{max}: left ventricular contraction velocity; dP/dt_{min}: left ventricular relaxation velocity; LV: left ventricle; LVEDP: left ventricular end diastolic pressure; Tau: index of left ventricular relaxation constant. Values are means \pm sem. *: $P < 0.05$ vs Ctrl.
doi:10.1371/journal.pone.0064711.t003

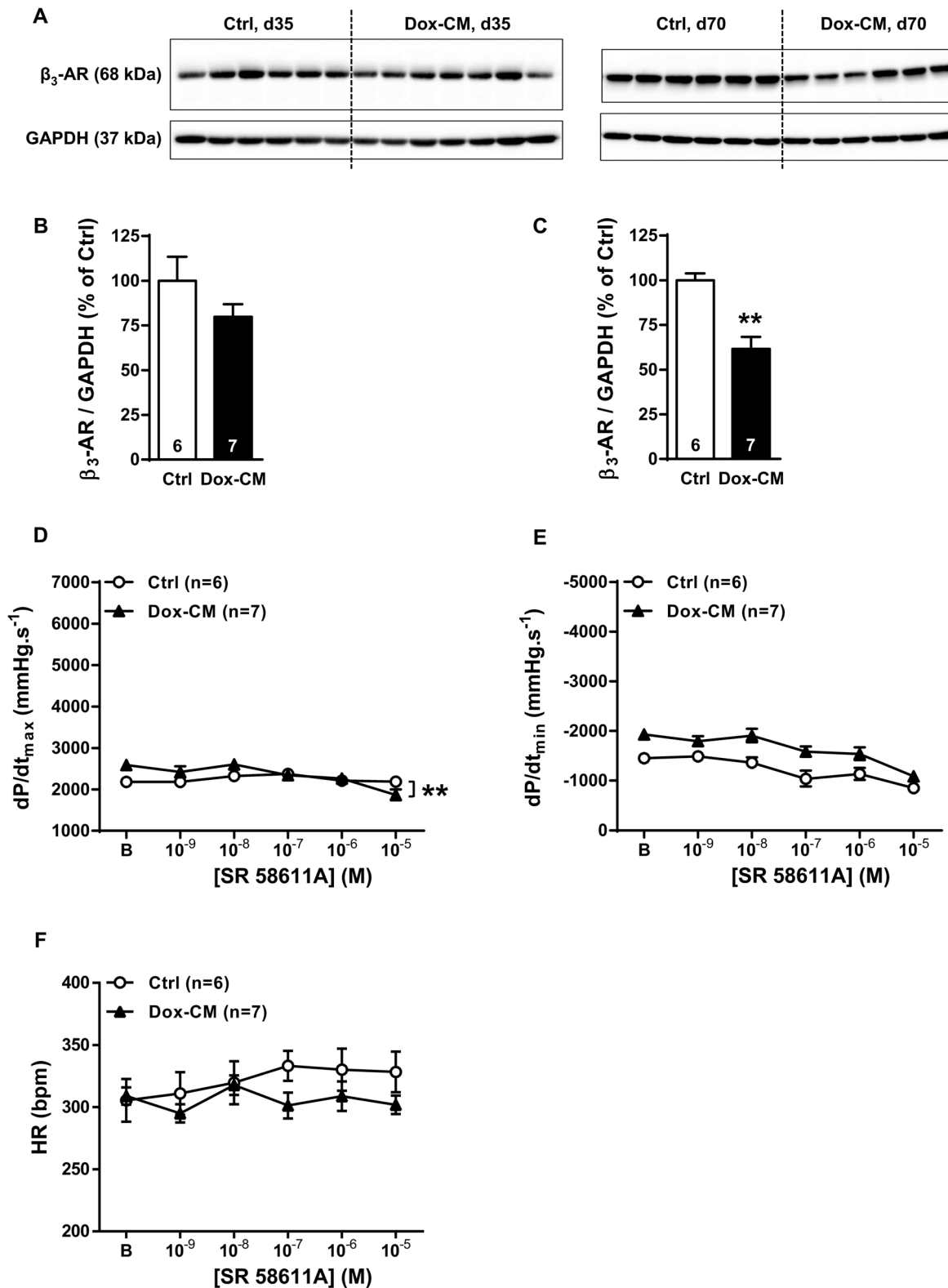


Figure 4. β_3 -AR expression and function in Dox-CM hearts. A. Representative β_3 -AR immunoblotting at days 35 (d35) and 70 (d70). B. β_3 -AR protein quantification at day 35. C. β_3 -AR protein quantification at day 70. Protein levels were quantified using Amersham ImageQuant RT-ECL camera (GE Healthcare). The band signals were assessed by densitometry with ImageQuant TL software (GE Healthcare) and a ratio to the corresponding GAPDH band intensity was calculated. D. Cardiac inotropic (dP/dt_{max}), E. lusitropic (dP/dt_{min}) and F. chronotropic (HR) effects of increasing concentrations of SR 58611A (10^{-9} to 10^{-5} M) were evaluated on isolated perfused hearts. **: $P < 0.001$ vs Ctrl. Ctrl: control, Dox-CM: Doxorubicin-induced cardiomyopathy. doi:10.1371/journal.pone.0064711.g004

end of Dox-treatment, the rat body weight increased again, but remained significantly lower than those of Ctrl rats, and reached a plateau from 5 weeks after the end of Dox-treatment (day 49; Figure 1A). In addition, Dox-CM rats became lethargic compared to Ctrl one.

The mortality rate was 25.0% at d35 and 58.3% at d70 in Dox-CM when no mortality was observed in Ctrl (Figure 1B). At d35, all surviving Dox-CM rats presented a hepatomegaly and 79.4% of them presented ascites (30.8 ± 5.8 mL), whereas at d70 no hepatomegaly was observed and ascites was present in 38.9% of Dox-CM rats (35.7 ± 4.9 mL). Whole heart and LV weights from Dox-CM rats were significantly smaller than those of Ctrl animals both at d35 and d70, and they were still smaller after normalization to the tibia length. However, heart/body weight ratios and LV/body weight ratios were similar between Ctrl and Dox-CM rats at d35 when it was increased in Dox-CM group compared to Ctrl at d70 (Table 2).

Cardiac Function Obtained by Echocardiography-Doppler

Echocardiography-Doppler analyses were performed at d35 and d70. Heart rate, measured before all echocardiographic acquisitions, was monitored in order to be similar between both groups (d35: Ctrl: 364 ± 6 bpm, Dox-CM: 371 ± 6 bpm, $P = 0.427$; d70: Ctrl: 368 ± 6 bpm, Dox-CM: 337 ± 17 bpm, $P = 0.079$). Representative images obtained by echocardiography in short axis view of a two-dimensionally directed M-mode at d35 are shown in Figure 2.

The dPWth decreased in Dox-CM compared to Ctrl hearts at d35 ($-9.5 \pm 3.3\%$, $P = 0.055$) and was significantly thinner at d70 ($-20.5 \pm 4.4\%$, $P < 0.001$) (Figure 3A). LVESV was similar in both groups at d35 as at d70 ($P = 0.199$ and $P = 0.116$, respectively). On the contrary, LVEDV was reduced in Dox-CM compared to Ctrl at d35 ($-12.6 \pm 1.9\%$, $P < 0.001$) as at d70 ($-21.7 \pm 8.7\%$, $P = 0.050$) (Figure 3B).

Compared to Ctrl, Dox-CM LVs were characterized at d35 by mild but significant decreases in LVEF ($-14.2 \pm 2.0\%$; $P < 0.001$) and LVSF ($-23.4 \pm 2.7\%$; $P < 0.001$), that were more pronounced at d70 ($-25.2 \pm 6.2\%$, $P < 0.001$ and $-34.9 \pm 7.4\%$, $P < 0.001$, respectively) (Figures 3C, D). Moreover, Dox-CM hearts presented an alteration in longitudinal deformation, since Sa was decreased at d35 ($-31.2 \pm 6.5\%$; $P = 0.001$) as at d70 ($-48.6 \pm 10.3\%$, $P < 0.001$) (Figure 3E) whereas radial deformation was only observed at d70 ($-38.7 \pm 4.9\%$, $P = 0.031$) (Figure 3F). In Dox-CM rats, IVRT value was significantly increased at d35 ($+25.7 \pm 3.4\%$, $P < 0.001$) as at d70 ($+31.1 \pm 10.6\%$, $P = 0.003$) (Figure 3G) albeit the LV filling pressures, evaluated by E/Ea ratio, were similar in Ctrl and Dox-CM rats at both d35 and d70 ($P = 0.776$ and $P = 0.071$, respectively) (Figure 3H).

Cardiac Function Obtained by Left Ventricle Catheterization

As our study consists to identify molecular target at early stage of Dox-CM, we only performed LV catheterization at d35. Basal heart rate, measured before all pressure acquisitions, was increased in Dox-CM rats compared to Ctrl ($P = 0.007$) (Table 3). Dox-CM rats presented a decreased Tau ($-10.0 \pm 2.2\%$; $P = 0.009$) albeit dP/dt_{max} and dP/dt_{min} were unchanged (Table 3). LVEDP was unchanged between both groups ($P = 0.216$).

β₃-adrenoceptor Expression and Function

Using western-blot, we detected β₃-AR protein at a band of 68 kDa (Figure 4A). At d35, the detected band presented a similar

intensity in Dox-CM and Ctrl ($P = 0.192$), whereas, at d70, β₃-ARs were down-expressed in Dox-CM hearts compared to Ctrl hearts ($-37.2 \pm 7.9\%$; $P < 0.001$) (Figures 4A–C). In Ctrl isolated heart, at d35, β₃-AR stimulation performed by cumulative increasing concentrations of SR 58611A produced no significant effect on heart rate and dP/dt_{max} at any concentration ($P = 0.239$ and $P = 0.385$, respectively) (Figures 4D, F) and decreased dP/dt_{min} only at the higher concentration of SR 58611A (10^{-5} M) ($P = 0.004$) (Figure 4E). Compared to Ctrl hearts, β₃-AR stimulation in Dox-CM hearts produced a significant decrease in dP/dt_{max} only at the higher concentration of SR 58611A (10^{-5} M) ($P < 0.001$) (Figure 4D) and had no effect on dP/dt_{min} nor heart rate ($P = 0.406$ and $P = 0.107$, respectively) (Figures 4E, F).

β₁-adrenoceptor Expression and Function

By western-blot, the antibody directed against β₁-AR detected a band at 72 kDa (Figure 5A) whose intensity was significantly decreased in Dox-CM LV at d35 by $-68.2 \pm 6.1\%$ ($P = 0.002$ vs Ctrl) (Figure 5B) and at d70 by $-75.3 \pm 14.0\%$ ($P < 0.001$ vs Ctrl) (Figure 5C). In Ctrl heart, at d35, β₁-AR stimulation induced a concentration-dependant increase in dP/dt_{max}, dP/dt_{min} and heart rate with a maximal effect observed at a concentration of 10^{-5} M ($P < 0.001$, each) (Figures 5D–F). The heart rate and the positive inotropic and lusitropic effects were unchanged in Dox-CM isolated hearts compared to Ctrl hearts ($P = 0.544$, $P = 0.772$ and $P = 0.667$, respectively) (Figures 5D–F).

β₂-adrenoceptor Expression and Function

By western-blot, the antibody directed against β₂-AR detected a band at 55 kDa (Figure 6A) whose intensity was significantly increased in Dox-CM LV at d35 by $+57.9 \pm 21.6\%$ ($P = 0.039$ vs Ctrl) (Figure 6B) and at d70 by $+173.7 \pm 35.1\%$ ($P < 0.001$ vs Ctrl) (Figure 6C). At d35, β₂-AR stimulation induced a similar concentration-dependant increase of heart rate between Ctrl and Dox-CM hearts ($P = 0.695$) (Figure 6F). In Ctrl isolated hearts, β₂-AR stimulation induced a concentration-dependant increase of dP/dt_{max} and dP/dt_{min} ($P < 0.001$ and $P = 0.005$, respectively) (Figures 6D, E) but at a lesser extent than β₁-AR one. In Dox-CM hearts, the maximal effects induced by β₂-AR stimulation on dP/dt_{max} and dP/dt_{min}, compared to Ctrl, were both increased by $+108.0 \pm 18.2\%$ ($P < 0.001$) and $+155.3 \pm 26.8\%$ ($P < 0.001$), respectively (Figures 6D, E), and reached a similar level than this produced by β₁-AR stimulation.

Gs Protein Expression and Adenylyl Cyclase Stimulation

By western-blot, we detected two bands for Gsα protein expression: a short one at 45 kDa and a long one at 52 kDa (Figure 7A). The expression of both forms was unchanged in Dox-CM hearts at both d35 and d70 (Figures 7B, C). In Ctrl and Dox-CM isolated hearts, at d35, forskolin induced a similar concentration-dependant increase of heart rate between Ctrl and Dox-CM hearts ($P = 0.941$) (Figure 7F). In Ctrl group, forskolin induced a concentration-dependant increase of dP/dt_{max} ($P < 0.001$) and dP/dt_{min} ($P = 0.010$) (Figures 7D, E). In Dox-CM isolated hearts compared to Ctrl, the forskolin effects on dP/dt_{max} and dP/dt_{min} were increased by $+43.2 \pm 10.3\%$ ($P = 0.004$) and $+61.1 \pm 10.7\%$ ($P = 0.002$), respectively (Figures 7D, E).

Gi Protein Expression and its Involvement in β₂-AR Cardiac Contractility

Giα₂ protein expression was detected by one band of 35 kDa (Figure 8A) whose intensity was similar both in Ctrl and Dox-CM hearts at d35 ($P = 0.184$ vs Ctrl) (Figure 8B), but was increased in

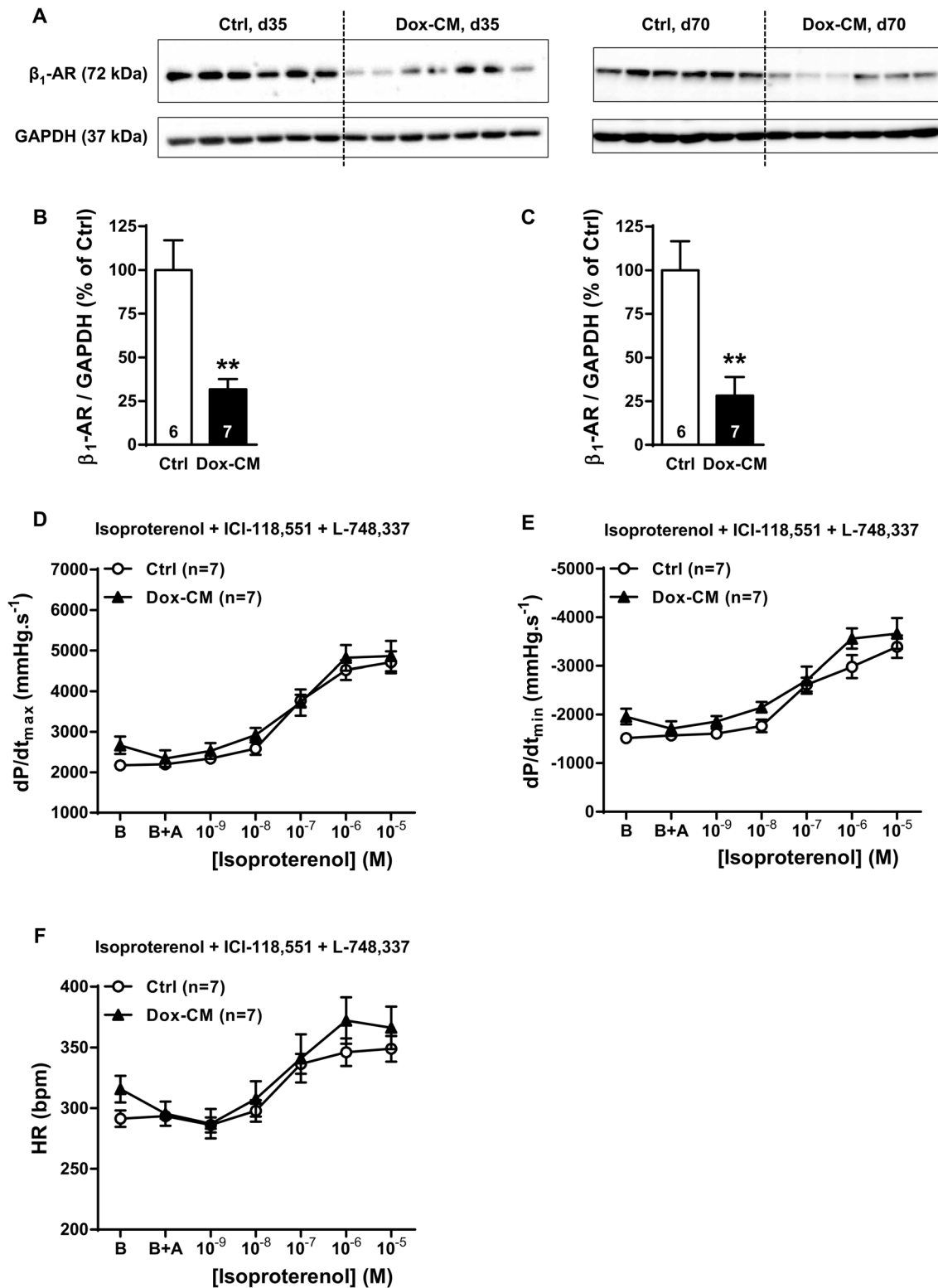


Figure 5. Impaired β_1 -AR expression in Dox-CM hearts was not associated to an impaired cardiac β_1 -AR function. A. Representative β_1 -AR immunoblotting at days 35 (d35) and 70 (d70). B. β_1 -AR protein quantification at day 35. C. β_1 -AR protein quantification at day 70. Protein levels were quantified using Amersham ImageQuant RT-ECL camera (GE Healthcare). The band signals were assessed by densitometry with ImageQuant TL software (GE Healthcare) and a ratio to the corresponding GAPDH band intensity was calculated. D. Cardiac inotropic (dP/dt_{max}), E. Lusitropic (dP/dt_{min}) and F. chronotropic (HR) effects of increasing concentrations of isoproterenol (10^{-9} to 10^{-5} M) in the presence of 10^{-6} M ICI-118,551 a β_2 -AR antagonist and 10^{-6} M of L-748,337 a β_3 -AR antagonist were evaluated on isolated perfused hearts. B: Baseline; B+A: Baseline in presence of antagonists. **: $P < 0.001$ vs Ctrl. Ctrl: control, Dox-CM: Doxorubicin-induced cardiomyopathy. doi:10.1371/journal.pone.0064711.g005

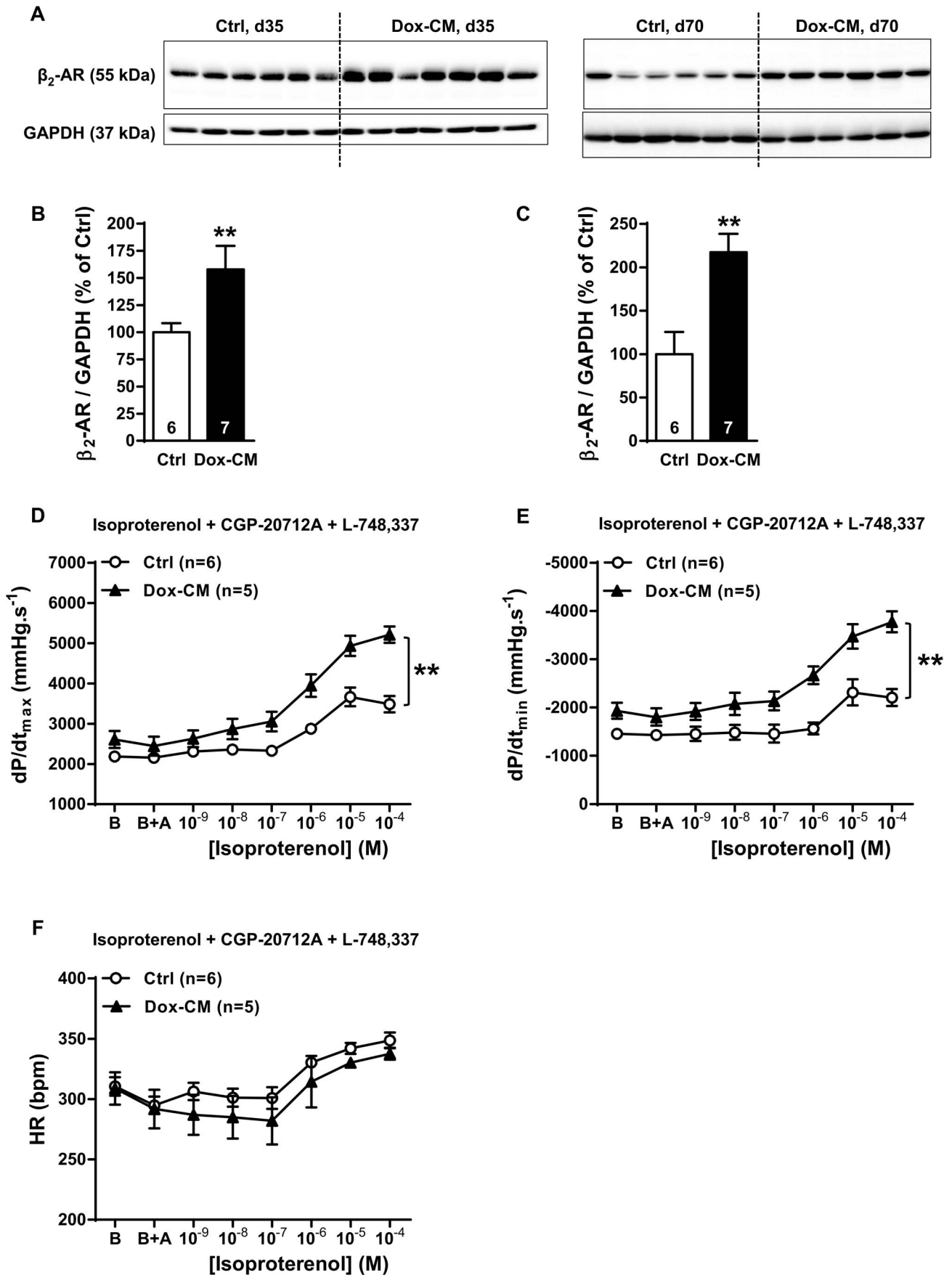


Figure 6. β_2 -AR expression and function are increased in Dox-CM hearts. A. Representative β_2 -AR immunoblotting at days 35 (d35) and 70 (d70). B. β_2 -AR protein quantification at day 35. C. β_2 -AR protein quantification at day 70. Protein levels were quantified using Amersham ImageQuant RT-ECL camera (GE Healthcare). The band signals were assessed by densitometry with ImageQuant TL software (GE Healthcare) and a ratio to the corresponding GAPDH band intensity was calculated. D. Cardiac inotropic (dP/dt_{max}), E. lusitropic (dP/dt_{min}) and F. chronotropic (HR) effects of increasing concentrations of isoproterenol (10^{-9} to 10^{-4} M) in presence of 10^{-6} M of CGP-20712A a β_1 -AR antagonist and 10^{-6} M of L-748,337 a β_3 -AR antagonist were evaluated on isolated perfused hearts. B: Baseline; B+A; Baseline the in presence of antagonists. **: $P < 0.001$ vs Ctrl; Ctrl: control, Dox-CM: Doxorubicin-induced cardiomyopathy. doi:10.1371/journal.pone.0064711.g006

Dox-CM hearts at d70 by $+118.1 \pm 37.6\%$ ($P = 0.009$ vs Ctrl) (Figure 8C). *Ex vivo*, at d35, Gi protein inhibition by PTX pretreatment produced no effect in heart rate in both groups ($P = 0.346$) (Figure 8F). PTX-pretreatment induced a significant increase of β_2 -AR stimulation in Ctrl isolated hearts (dP/dt_{max} : $+64.4 \pm 9.8\%$; $P < 0.001$; dP/dt_{min} : $+128.0 \pm 20.8\%$; $P < 0.001$) (Figures 8D, E) but induced no change of these two parameters in Dox-CM hearts ($P = 0.173$ and $P = 0.451$, respectively) (Figures 8D, E).

Discussion

This study demonstrated for the first time in Dox-cardiotoxicity, β_2 -AR expression was increased at the early stage of the pathology, with an increase of β_2 -AR-induced contractility. Furthermore, β_1 -AR function was preserved in spite of decreased β_1 -AR protein expression and could be explained by an increase of AC expression and/or activity as illustrated by an increased forskolin-induced contractility in isolated hearts from Dox-CM rats.

In our study, the body weight of Dox-CM rats was smaller than in Ctrl one as previously described by other studies [8,24]. This has been related to a decrease in food consumption [25,26]. In our experimental conditions, we have, 35 days after the beginning of Dox-treatment, 25% of mortality and rats presented a large amount of ascites. Those observations were in agreement with other studies that reported a mortality rate fluctuating between 19% and 45% [27,28] and a volume of ascites generally varying from 30 mL to 140 mL [24,28–30]. However, as Dox induced a multi-organ toxicity, it could be not excluded that mortality and ascites observed in rats could be due, at least in part, to liver and kidney damages. Seventy days after the beginning of Dox-treatment, mortality rate increased to 58% and ascites was still observed. Very few studies reported long term effects of Dox-treatment and data on mortality and ascites are very heterogeneous. Whereas a study observed 50% mortality rate 6 weeks after the last Dox-injection, associated with a very large amount of ascites [25] others did not observed mortality eight weeks after the last Dox-injection [11]. Also, others did not reported mortality and observed a decrease in ascites amount between days 40 and 70 [26].

During echocardiographic acquisitions, heart rate was monitored in order to have similar heart rate in both groups, allowing a comparison of echocardiographic parameters. At d35, Dox-CM rats presented a slight alteration of systolic function as illustrated by a mild decrease in LVEF and LVSF and in LV longitudinal deformation. Dox-CM rats presented also a mild diastolic dysfunction as suggested by the increased IVRT and Tau values. At d70, decreases in LVEF, LVSF and LV longitudinal deformation were exacerbated whereas diastolic dysfunction was unchanged. As diastolic dysfunction frequently occurs before systolic dysfunction [31–33], we could suggest that in our animal model, at d35, systolic function just began to be altered, meaning that this model corresponds to an early chronic Dox-cardiotoxicity. It is important to note that our results are very close to that observed in women who received anthracycline-treatment for breast cancer. Indeed, these patients had preserved LVEF

compared to controls but a significantly reduced longitudinal strain with preserved radial contractility [34].

In human, Dox administered to adults (for breast cancer, for example) is well known to induce chronic cardiotoxicity where cardiac morphologic and functional alterations are close to those of dilated cardiomyopathy [3]. However, when administered in children, Dox can induce restrictive cardiomyopathy with normal LV dimensions [35]. Those findings, are consistent with those of other long-term follow-up studies conducted in other groups of anthracycline-treated childhood cancer survivors [36]. In our study, Dox was administered to young rats (7 week-old). At d35, we observed diastolic dysfunction with normal systolic function that could support the hypothesis of a restrictive-cardiomyopathy. At d70, the development of systolic dysfunction could suggest restrictive cardiomyopathy worsening with increase LV dimensions. Indeed, although LVEDDs were not statistically different between Ctrl and Dox-CM rats at d70, it is important to note that LV dPWth was significantly decreased in Dox-CM compared to Ctrl rats, strengthening the notion of LV morphologic changes in those rats. We could hypothesize that a period of 56 days post-treatment was a too short duration of the disease evolution to observe a significant LV dilation in Dox-CM rats. Indeed, in human HF, the dilation is considered as the last stage of ischemic or non ischemic cardiomyopathy evolution as in Dox-CM. In this latter disease, it is well known that cardiomyopathy and thus LV dilation occur up to decades after exposure [37].

In our Dox-CM model, we reported a remodeling in β -AR expression and function. Three weeks after last Dox-injection (d35), β_3 -AR protein expression was unchanged and a slight negative inotropic effect was obtained in Dox-CM hearts at the higher concentration of SR 58611A (10^{-5} M). Our data suggest that in early chronic Dox-cardiotoxicity, β_3 -AR could not play a major role in the cardiac alterations. At a later stage (d70), we observed a decreased β_3 -AR protein expression in Dox-CM hearts albeit another team reported an overexpression of β_3 -AR protein at the same stage [11]. Several hypotheses could explain those discrepancies. First, the rat strain used in the study is different (Wistar vs Sprague-Dawley) and several studies reported that protein expression could be different between Sprague-Dawley and Wistar rats [38,39] albeit no study compared β -AR subtypes expression between these two rat strains. Second, in the Sun's study, cardiac β -ARs expressions were assessed in Ctrl rats compared to Dox-treated rats which were also Sham-castrated (scrotum incision); no surgery being performed in Ctrl rats. Therefore, β -AR protein expressions were assessed in a Dox-CM model different from our one used in our study.

In our Dox-CM model, β_1 -AR protein expression was decreased at both stages. This result is in agreement with those reported for β_1 -AR protein expression both in rabbits [40] and in rats [8,11]. Surprisingly, albeit a decreased β_1 -AR expression at d35, the cardiac β_1 -AR responses were preserved. Several hypotheses could explain this feature. Firstly, a β_1 -AR reserve could be present and recruited in such conditions and, secondly, an increase in β_1 -AR signaling pathway can be evoked. We showed that Dox-treatment did not change Gs α protein expression, as it was reported in other study [8,11], but increased

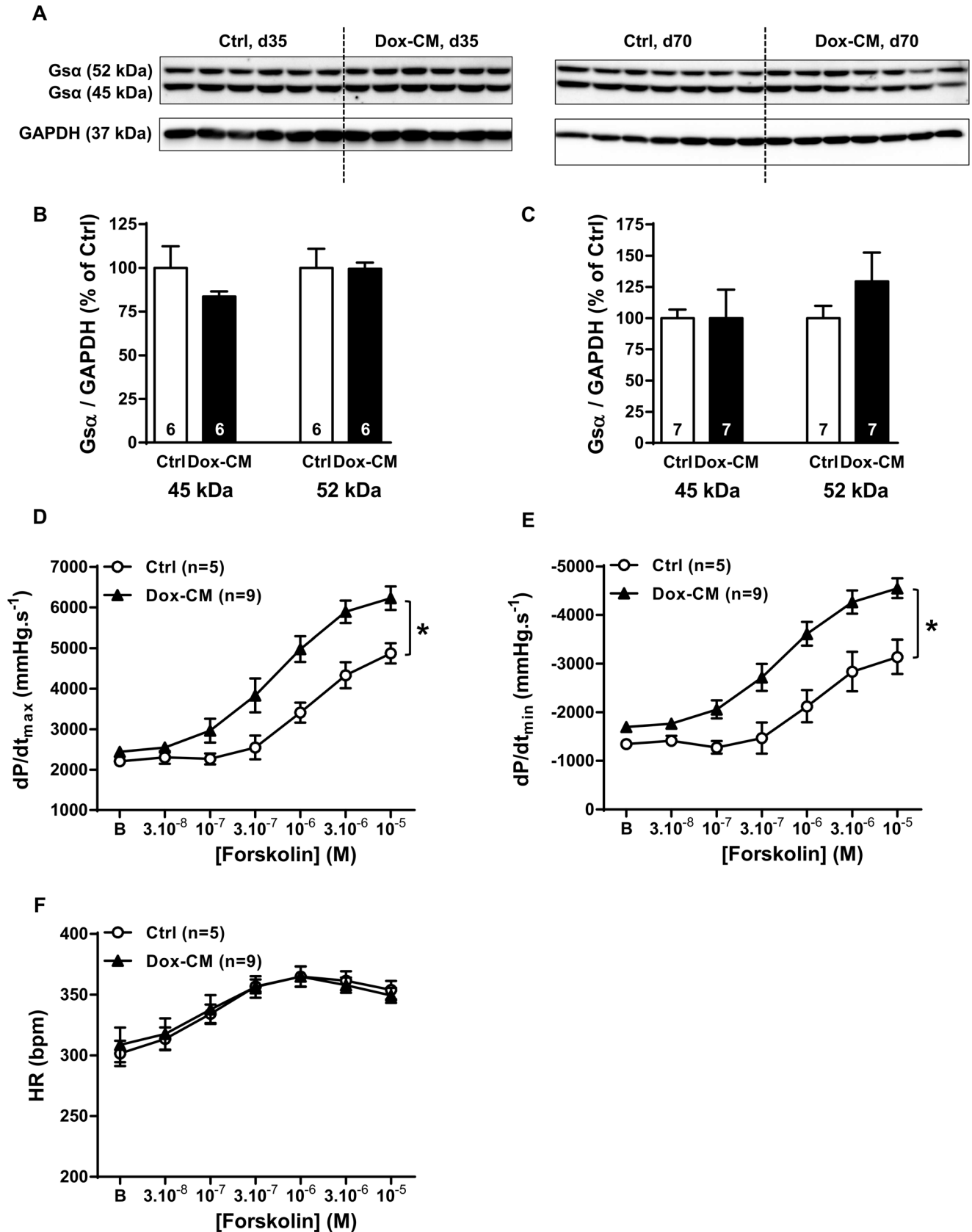


Figure 7. Gsα protein expression and forskolin response. **A.** Representative Gsα immunoblotting at days 35 (d35) and 70 (d70). **B.** Gsα protein quantification at day 35. **C.** Gsα protein quantification at day 70. Protein levels were quantified using Amersham ImageQuant RT-ECL camera (GE Healthcare). The band signals were assessed by densitometry with ImageQuant TL software (GE Healthcare) and a ratio to the corresponding GAPDH band intensity was calculated. **D.** Cardiac inotropic (dP/dt_{max}), **E.** lusitropic (dP/dt_{min}) and **F.** chronotropic (HR) effects of increasing concentrations of the adenylyl cyclase activator forskolin (3.10⁻⁸ to 10⁻⁵ M) were evaluated on isolated perfused hearts. *: P<0.05 vs Ctrl. Ctrl: control, Dox-CM: Doxorubicin-induced cardiomyopathy. doi:10.1371/journal.pone.0064711.g007

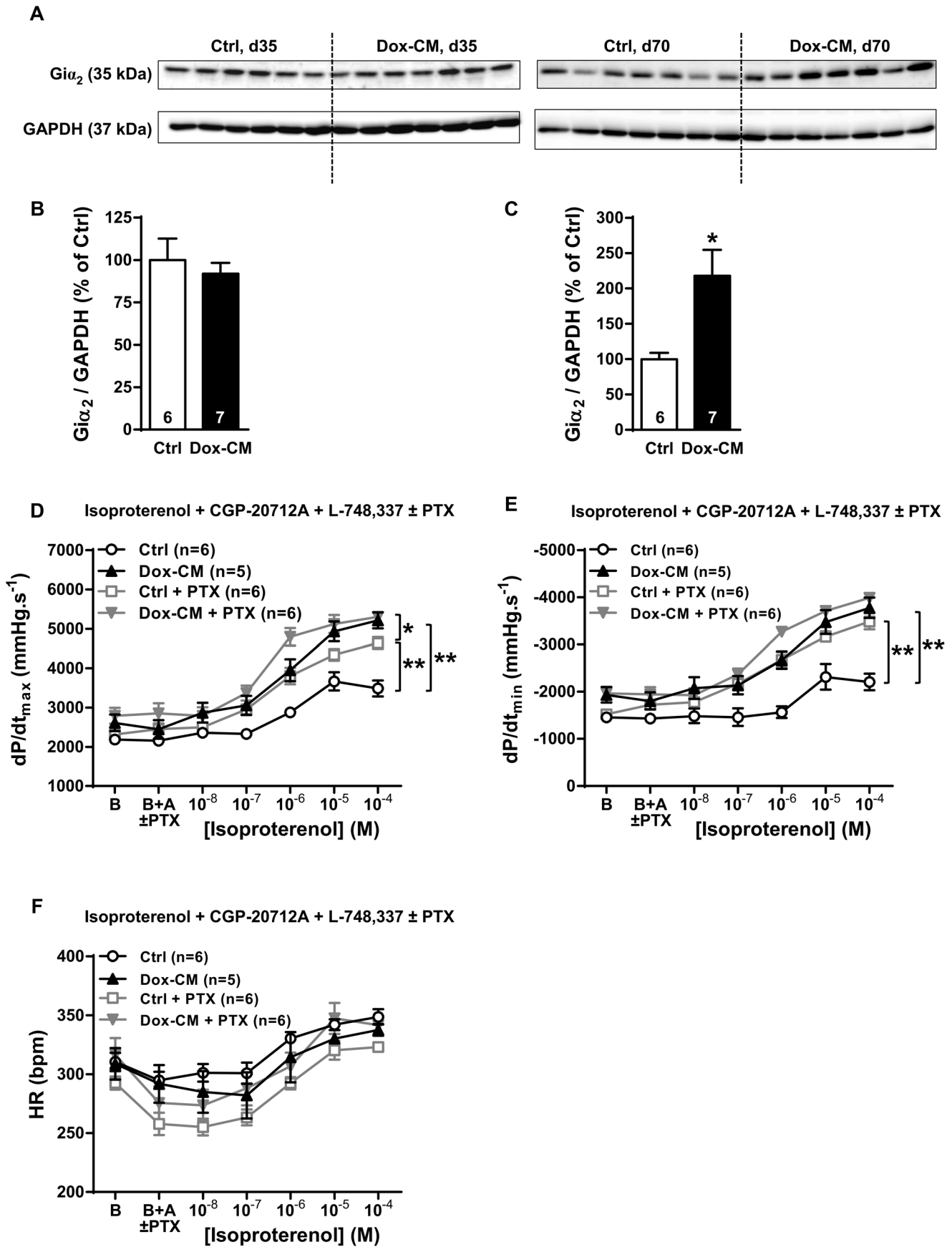


Figure 8. Gi protein expression and involvement in β_2 -AR cardiac contractility. **A.** Representative $G\alpha_2$ immunoblotting at days 35 (d35) and 70 (d70). **B.** $G\alpha_2$ protein quantification at day 35. **C.** $G\alpha_2$ protein quantification at day 70. Protein levels were quantified using Amersham ImageQuant RT-ECL camera (GE Healthcare). The band signals were assessed by densitometry with ImageQuant TL software (GE Healthcare) and a ratio to the corresponding GAPDH band intensity was calculated. **D.** Cardiac inotropic (dP/dt_{max}), **E.** lusitropic (dP/dt_{min}) and **F.** chronotropic (HR) effects of increasing concentrations of isoproterenol (10^{-9} to 10^{-4} M) in the presence of 10^{-6} M of CGP-20712A and 10^{-6} M of L-748,337 were evaluated on isolated perfused hearts pre-treated or not with $4 \mu\text{g}\cdot\text{L}^{-1}$ of pertussis toxin (PTX) a Gi protein inhibitor. B: Baseline; B+A; Baseline in the presence of antagonists. *: $P < 0.05$ vs Ctrl; **: $P < 0.001$ vs Ctrl. Ctrl: control, Dox-CM: Doxorubicin-induced cardiomyopathy. doi:10.1371/journal.pone.0064711.g008

forskolin response, suggesting an increase in AC expression and/or activity. This surprising data contrasts with other studies which reported a decreased AC activity [41,42] or no change [43]. However, those differences seem to be due to the cardiotoxicity level since the Dox cumulative doses used were 24, 24.75 and $6 \text{ mg}\cdot\text{kg}^{-1}$, respectively. Thus, the increased AC response to forskolin observed in our study could be a compensatory mechanism at early stage of Dox-cardiotoxicity to maintain cardiac contractility and could explain, at least in part, the preserved β_1 -AR response. However, as β_1 -ARs are involved in pro-apoptotic effects, β_1 -AR could be also responsible for some Dox cardiotoxic effects as previously suggested [9,10].

Finally, we reported, for the first time, in chronic Dox-cardiotoxicity, a β_2 -AR protein overexpression. At d35, in Ctrl isolated heart, specific β_2 -AR stimulation induced positive inotropic and lusitropic responses but to a lesser extent than β_1 -AR one. This lower response could be explained by a more compartmentalized cAMP signaling of β_2 -AR [44]. Surprisingly, in Dox-CM hearts, β_2 -AR inotropic effect was increased and reached a similar level than β_1 -AR stimulation. This increase could be due to several mechanisms. Firstly, we show that β_2 -AR protein expression was increased in Dox-CM LV and could lead to an increased β_2 -AR response. Secondly, cardiac β_2 -AR could be linked both to Gs and Gi proteins [45,46]. In Dox-CM LV, $G\alpha_2$ protein expression was not modified at d35 but it was overexpressed at d70 of Dox-CM, as reported previously at this latter stage by Sun *et al.* [11]. Surprisingly, at d35, in Ctrl hearts, the Gi inhibition by PTX allowed to increase β_2 -AR response in order to reach the same level that obtained in Dox-CM in the absence of PTX treatment, whereas Gi inhibition in Dox-CM hearts slightly increased β_2 -AR response. These data suggest that, in Dox-CM, β_2 -AR was mainly linked to Gs.

To know whether enhanced β_2 -AR/Gs signaling observed in our study is a beneficial compensatory mechanism or a detrimental effect is still to be determined. To support the hypothesis of a beneficial effect of β_2 -AR agonist, it has been shown that β_2 -AR/Gi signaling can mediate cardiac protective effects by activating cell surviving pathway [10,47,48], and also *in vivo* studies reported beneficial effects of β_2 -agonist therapy in

HF [49–54]. Concerning a putative detrimental effect of β_2 -AR, it could be proposed to use β_2 -AR blocker. However, it is important to note that β_2 -AR antagonists by blocking other physiological functions regulated by β_2 -AR, could also have detrimental effects: (i) a vasoconstriction because β_2 -AR is one of the most important vascular β -AR subtype whose activation induces a vasodilation in several vascular beds (including coronary vessels), (ii) a bronchoconstriction due to the reduction of bronchodilation induced by pulmonary β_2 -AR,...

Thus, we rather suggest that further experiments must be performed to identify the most suitable effector of the cardiac β_2 -AR pathway. Then, according to the results of this next important study, we hope that we could propose a new therapeutic target for Dox-CM.

In conclusion, we have shown for the first time in rat Dox-CM, an increase of β_2 -AR protein expression at early stage of the pathology, associated to an increased contractility. Furthermore, we observed a preserved β_1 -AR function albeit β_1 -AR was reduced. Clinical studies have suggested no beneficial effect of metoprolol, a β_1 -AR blocker, in Dox-treated lymphoma patients [15] but a beneficial effect of nebivolol, a β_1 -AR blocker associated to a β_3 -AR agonistic properties against anthracycline-induced cardiomyopathy in patients with breast cancer [55]. However, the clinical roles of β_2 -AR remain to elucidate in order to determine whether β_2 -AR activation or blockade could prevent cardiac alterations due to anthracycline.

Acknowledgments

We thank Chrystelle Bailly, Stéphanie Lemarchand-Mindé, Amandine Lefebvre and Patricia Charpentier for animal care, and Mortéza Erfanian for its technical assistance.

Author Contributions

Conceived and designed the experiments: NM BR CG. Performed the experiments: NM NP AG BL. Analyzed the data: NM NP AG BL BR CG. Contributed reagents/materials/analysis tools: JNT. Wrote the paper: NM BL BR CG.

References

- Connors JM (2005) State-of-the-art therapeutics: Hodgkin's lymphoma. *J Clin Oncol* 23: 6400–6408.
- Grimer R, Judson I, Peake D, Seddon B (2010) Guidelines for the management of soft tissue sarcomas. *Sarcoma* 2010: 506182.
- Ferreira AL, Matsubara LS, Matsubara BB (2008) Anthracycline-induced cardiotoxicity. *Cardiovasc Hematol Agents Med Chem* 6: 278–281.
- Nakamura T, Ueda Y, Juan Y, Katsuda S, Takahashi H, et al. (2000) Fas-mediated apoptosis in adriamycin-induced cardiomyopathy in rats: *In vivo* study. *Circulation* 102: 572–578.
- Ueno M, Kakinuma Y, Yuhki K, Murakoshi N, Iemitsu M, et al. (2006) Doxorubicin induces apoptosis by activation of caspase-3 in cultured cardiomyocytes *in vitro* and rat cardiac ventricles *in vivo*. *J Pharmacol Sci* 101: 151–158.
- Takemura G, Fujiwara H (2007) Doxorubicin-induced cardiomyopathy from the cardiotoxic mechanisms to management. *Prog Cardiovasc Dis* 49: 330–352.
- Chatterjee K, Zhang J, Honbo N, Karliner JS (2010) Doxorubicin cardiomyopathy. *Cardiology* 115: 155–162.
- Kenk M, Thackeray JT, Thorn SL, Dhimi K, Chow BJ, et al. (2010) Alterations of pre- and postsynaptic noradrenergic signaling in a rat model of adriamycin-induced cardiotoxicity. *J Nucl Cardiol* 17: 254–263.
- Bernstein D, Fajardo G, Zhao M, Urashima T, Powers J, et al. (2005) Differential cardioprotective/cardiotoxic effects mediated by beta-adrenergic receptor subtypes. *Am J Physiol Heart Circ Physiol* 289: H2441–2449.
- Fajardo G, Zhao M, Powers J, Bernstein D (2006) Differential cardiotoxic/cardioprotective effects of beta-adrenergic receptor subtypes in myocytes and fibroblasts in doxorubicin cardiomyopathy. *J Mol Cell Cardiol* 40: 375–383.
- Sun J, Fu L, Tang X, Han Y, Ma D, et al. (2011) Testosterone modulation of cardiac beta-adrenergic signals in a rat model of heart failure. *Gen Comp Endocrinol* 172: 518–525.
- Dery AS, Hamilton LA, Starr JA (2011) Nebivolol for the treatment of heart failure. *Am J Health Syst Pharm* 68: 879–886.
- Rozec B, Erfanian M, Laurent K, Trochu JN, Gauthier C (2009) Nebivolol, a vasodilating selective beta(1)-blocker, is a beta(3)-adrenoceptor agonist in the nonfailing transplanted human heart. *J Am Coll Cardiol* 53: 1532–1538.

14. Kalay N, Basar E, Ozdogru I, Er O, Cetinkaya Y, et al. (2006) Protective effects of carvedilol against anthracycline-induced cardiomyopathy. *J Am Coll Cardiol* 48: 2258–2262.
15. Georgakopoulos P, Roussou P, Matsakas E, Karavidas A, Anagnostopoulos N, et al. (2010) Cardioprotective effect of metoprolol and enalapril in doxorubicin-treated lymphoma patients: a prospective, parallel-group, randomized, controlled study with 36-month follow-up. *Am J Hematol* 85: 894–896.
16. Senba M, Buziba N, Mori N, Morimoto K, Nakamura T (2011) Increased prevalence of Kaposi sarcoma-associated herpesvirus in the Kaposi sarcoma-endemic area of western Kenya in 1981–2000. *Acta Virol* 55: 161–164.
17. Cardinale D, Colombo N, Lamantia G, Colombo N, Civelli M, et al. (2010) Anthracycline-induced cardiomyopathy: clinical relevance and response to pharmacologic therapy. *J Am Coll Cardiol* 55: 213–220.
18. Schiller NB, Shah PM, Crawford M, DeMaria A, Devereux R, et al. (1989) Recommendations for quantitation of the left ventricle by two-dimensional echocardiography. American Society of Echocardiography Committee on Standards, Subcommittee on Quantitation of Two-Dimensional Echocardiograms. *J Am Soc Echocardiogr* 2: 358–367.
19. Liu J, Rigel DF (2009) Echocardiographic examination in rats and mice. *Methods Mol Biol* 573: 139–155.
20. Mulvagh S, Quinones MA, Kleiman NS, Cheirif J, Zoghbi WA (1992) Estimation of left ventricular end-diastolic pressure from Doppler transmitral flow velocity in cardiac patients independent of systolic performance. *J Am Coll Cardiol* 20: 112–119.
21. Popovic ZB, Benjam C, Bian J, Mal N, Drinko J, et al. (2007) Speckle-tracking echocardiography correctly identifies segmental left ventricular dysfunction induced by scarring in a rat model of myocardial infarction. *Am J Physiol Heart Circ Physiol* 292: H2809–2816.
22. Rautureau Y, Toumaniantz G, Serpillon S, Jourdon P, Trochu JN, et al. (2002) Beta 3-adrenoceptor in rat aorta: molecular and biochemical characterization and signalling pathway. *Br J Pharmacol* 137: 153–161.
23. Bian JS, Zhang WM, Xia Q, Wong TM (1998) Phospholipase C inhibitors attenuate arrhythmias induced by kappa-receptor stimulation in the isolated rat heart. *J Mol Cell Cardiol* 30: 2103–2110.
24. Lou H, Danelisen I, Singal PK (2004) Cytokines are not upregulated in adriamycin-induced cardiomyopathy and heart failure. *J Mol Cell Cardiol* 36: 683–690.
25. Tong J, Ganguly PK, Singal PK (1991) Myocardial adrenergic changes at two stages of heart failure due to adriamycin treatment in rats. *Am J Physiol* 260: H909–916.
26. Ghibu S, Delemeasure S, Richard C, Guiland JC, Martin L, et al. (2012) General oxidative stress during doxorubicin-induced cardiotoxicity in rats: absence of cardioprotection and low antioxidant efficiency of alpha-lipoic acid. *Biochimie* 94: 932–939.
27. Iliskovic N, Singal PK (1997) Lipid lowering: an important factor in preventing adriamycin-induced heart failure. *Am J Pathol* 150: 727–734.
28. Morishima I, Matsui H, Mukawa H, Hayashi K, Toki Y, et al. (1998) Melatonin, a pineal hormone with antioxidant property, protects against adriamycin cardiomyopathy in rats. *Life Sci* 63: 511–521.
29. Danelisen I, Palace V, Lou H, Singal PK (2002) Maintenance of myocardial levels of vitamin A in heart failure due to adriamycin. *J Mol Cell Cardiol* 34: 789–795.
30. Iliskovic N, Panagia V, Slezak J, Kumar D, Li T, et al. (1997) Adriamycin depresses in vivo and in vitro phosphatidylethanolamine N-methylation in rat heart sarcolemma. *Mol Cell Biochem* 176: 235–240.
31. Nagy AC, Cserep Z, Tolnay E, Nagykalnai T, Forster T (2008) Early diagnosis of chemotherapy-induced cardiomyopathy: a prospective tissue Doppler imaging study. *Pathol Oncol Res* 14: 69–77.
32. Stoddard MF, Seeger J, Liddell NE, Hadley TJ, Sullivan DM, et al. (1992) Prolongation of isovolumetric relaxation time as assessed by Doppler echocardiography predicts doxorubicin-induced systolic dysfunction in humans. *J Am Coll Cardiol* 20: 62–69.
33. Tassan-Mangina S, Codorean D, Metivier M, Costa B, Himmerlin C, et al. (2006) Tissue Doppler imaging and conventional echocardiography after anthracycline treatment in adults: early and late alterations of left ventricular function during a prospective study. *Eur J Echocardiogr* 7: 141–146.
34. Ho E, Brown A, Barrett P, Morgan RB, King G, et al. (2010) Subclinical anthracycline- and trastuzumab-induced cardiotoxicity in the long-term follow-up of asymptomatic breast cancer survivors: a speckle tracking echocardiographic study. *Heart* 96: 701–707.
35. Lipshultz SE, Lipsitz SR, Sallan SE, Dalton VM, Mone SM, et al. (2005) Chronic progressive cardiac dysfunction years after doxorubicin therapy for childhood acute lymphoblastic leukemia. *J Clin Oncol* 23: 2629–2636.
36. Brouwer CA, Gietema JA, van den Berg MP, Bink-Boelkens MT, Elzenga NJ, et al. (2006) Long-term cardiac follow-up in survivors of a malignant bone tumour. *Ann Oncol* 17: 1586–1591.
37. Steinherz IJ, Steinherz PG, Tan CT, Heller G, Murphy ML (1991) Cardiac toxicity 4 to 20 years after completing anthracycline therapy. *JAMA* 266: 1672–1677.
38. Kishida T, Muto S, Hayashi M, Tsutsui M, Tanaka S, et al. (2008) Strain differences in hepatic cytochrome P450 1A and 3A expression between Sprague-Dawley and Wistar rats. *J Toxicol Sci* 33: 447–457.
39. Jamesdaniel S, Ding D, Kermany MH, Jiang H, Salvi R, et al. (2009) Analysis of cochlear protein profiles of Wistar, Sprague-Dawley, and Fischer 344 rats with normal hearing function. *J Proteome Res* 8: 3520–3528.
40. Dhein S, Garbade J, Rouabah D, Abraham G, Ungemach FR, et al. (2006) Effects of autologous bone marrow stem cell transplantation on beta-adrenoceptor density and electrical activation pattern in a rabbit model of non-ischemic heart failure. *J Cardiothorac Surg* 1: 17.
41. Calderone A, de Champlain J, Rouleau JL (1991) Adriamycin-induced changes to the myocardial beta-adrenergic system in the rabbit. *J Mol Cell Cardiol* 23: 333–342.
42. Nagami K, Yoshikawa T, Suzuki M, Wainai Y, Anzai T, et al. (1997) Abnormal beta-adrenergic transmembrane signaling in rabbits with adriamycin-induced cardiomyopathy. *Jpn Circ J* 61: 249–255.
43. Fu LX, Bergh CH, Hoebeke J, Liang QM, Sjogren KG, et al. (1991) Effect of metoprolol on activity of beta-adrenoceptor coupled to guanine nucleotide binding regulatory proteins in adriamycin-induced cardiotoxicity. *Basic Res Cardiol* 86: 117–126.
44. Nikolaev VO, Bunemann M, Schmitteckert E, Lohse MJ, Engelhardt S (2006) Cyclic AMP imaging in adult cardiac myocytes reveals far-reaching beta1-adrenergic but locally confined beta2-adrenergic receptor-mediated signaling. *Circ Res* 99: 1084–1091.
45. Pavoinc C, Defer N (2005) The cardiac beta2-adrenergic signalling a new role for the cPLA2. *Cell Signal* 17: 141–152.
46. Xiao RP, Zhu W, Zheng M, Cao C, Zhang Y, et al. (2006) Subtype-specific alpha1- and beta-adrenoceptor signaling in the heart. *Trends Pharmacol Sci* 27: 330–337.
47. Zhu WZ, Zheng M, Koch WJ, Lefkowitz RJ, Kobilka BK, et al. (2001) Dual modulation of cell survival and cell death by beta(2)-adrenergic signaling in adult mouse cardiac myocytes. *Proc Natl Acad Sci U S A* 98: 1607–1612.
48. DeGeorge BR, Jr., Gao E, Boucher M, Vinge LE, Martini JS, et al. (2008) Targeted inhibition of cardiomyocyte Gi signaling enhances susceptibility to apoptotic cell death in response to ischemic stress. *Circulation* 117: 1378–1387.
49. Ahmet I, Krawczyk M, Heller P, Moon C, Lakatta EG, et al. (2004) Beneficial effects of chronic pharmacological manipulation of beta-adrenoceptor subtype signaling in rodent dilated ischemic cardiomyopathy. *Circulation* 110: 1083–1090.
50. Ahmet I, Krawczyk M, Zhu W, Woo AY, Morrell C, et al. (2008) Cardioprotective and survival benefits of long-term combined therapy with beta2 adrenoceptor (AR) agonist and beta1 AR blocker in dilated cardiomyopathy postmyocardial infarction. *J Pharmacol Exp Ther* 325: 491–499.
51. Ahmet I, Morrell C, Lakatta EG, Talan MI (2009) Therapeutic efficacy of a combination of a beta1-adrenoceptor (AR) blocker and beta2-AR agonist in a rat model of postmyocardial infarction dilated heart failure exceeds that of a beta1-AR blocker plus angiotensin-converting enzyme inhibitor. *J Pharmacol Exp Ther* 331: 178–185.
52. Chakir K, Daya SK, Aiba T, Tunin RS, Dimaano VL, et al. (2009) Mechanisms of enhanced beta-adrenergic reserve from cardiac resynchronization therapy. *Circulation* 119: 1231–1240.
53. Chakir K, Depy C, Dimaano VL, Zhu WZ, Vanderheyden M, et al. (2011) Galpha-biased beta2-adrenergic receptor signaling from restoring synchronous contraction in the failing heart. *Sci Transl Med* 3: 100ra188.
54. Zhu W, Petrashevskaya N, Ren S, Zhao A, Chakir K, et al. (2012) Gi-biased beta2AR signaling links GRK2 upregulation to heart failure. *Circ Res* 110: 265–274.
55. Kaya MG, Ozkan M, Gunbakmaz O, Akkaya H, Kaya EG, et al. (2012) Protective effects of nebivolol against anthracycline-induced cardiomyopathy: A randomized control study. *Int J Cardiol*.